Preliminary marine gravity field from HY-2A/GM altimeter data

Qiankun Liu[1, 2], Ke Xu[1]*, Maofei Jiang[1], Jiaming Wang[1, 2]

[1] The CAS Key Laboratory of Microwave Remote Sensing, National Space Science Center, Chinese Academy of Sciences (CAS), Beijing 100190, China

[2] University of Chinese Academy of Sciences, Beijing 100049, China

Abstract

HY-2A (Haiyang-2A), launched in 2011, is the first ocean dynamic environment satellite of China and is equipped with a radar altimeter as one of the primary payloads. HY-2A shifted the drift orbit in March 2016 and has been accumulating geodetic mission (GM) data for more than three years with 168-day cycle. In this paper, we present the preliminary gravity field inverted by the HY-2A/GM data from March 2016 to December 2017 near Taiwan (21°–26°N, 119°–123°E). The gravity anomaly is computed by Inverse Vening Meinesz (IVM) formula with a one-dimensional FFT method during remove-restore procedure with the EGM2008 gravity model as the reference field. For comparison, CryoSat-2 altimeter data are used to inverse the gravity field near Taiwan Island by the same method. Comparing with the gravity field derived from CryoSat-2, a good agreement between the two data sets is found. The global ocean gravity models and National Geophysical Data Center (NGDC) shipboard gravity data also are used to assess the performance of HY-2A/GM data. The evaluations show that HY-2A and CryoSat-2 are at the same level in terms of gravity field recovery and the HY-2A/GM altimeter-derived gravity field has an accuracy of 2.922 mGal. Therefore, we can believe that HY-2A will be a new reliable data source for marine gravity field inversion and has the potentiality to improve the accuracy and resolution of the global marine gravity field.

Key words: HY-2A, radar altimeter, geodetic mission, marine gravity anomaly, inversion

Citation: Liu Qiankun, Xu Ke, Jiang Maofei, Wang Jiaming. 2020. Preliminary marine gravity field from HY-2A/GM altimeter data. Acta Oceanologica Sinica, 39(7): 127–134, doi: 10.1007/s13131-020-1610-4

1 Introduction

The satellite radar altimeter is an important microwave remote sensor. The radar altimeter loaded on the satellite sends radar pulse signals to the sea surface and receives echo signals. Through ground data processing, the sea surface height (SSH), significant wave height and wind speed measurements can be obtained. Retrieving the ocean gravity field using altimeter SSH data is one of the main applications of satellite altimeters. This work was first demonstrated with GEO-3 data by Rapp (1979). Marine gravity fields and geoids obtained from GEO-3, Seasat and GEOSAT exact repetitive mission (ERM) data were given (Haxby et al., 1983; Rapp, 1986; Sandwell and McAdoo, 1988). Due to the sparse ground track of ERM data, these inversion results were limited to spatial resolutions with wavelengths longer than 50–100 km. The emergence of GEOSAT geodetic mission (GM) data represented an important milestone: a single satellite altimeter can fully map high-resolution ocean geoids and ocean gravity fields. Such a marine gravity field was first introduced by McAdoo and Marks (1992). During 40 years, dozens of altimetry satellites have been launched. Among the altimetry satellites, only a few satellites had geodetic data, such as GEOSAT, ERS-1, CryoSat-2, Jason-1, Jason-2, SARAL/AltiKa, which had greatly facilitated the high-resolution ocean gravity inversion (Sandwell and Smith, 1997, 2009; Andersen and Knudsen, 1998; Hwang et al., 1998, 2002; Andersen et al., 2010, 2014; Sandwell et al., 2013; Hsiao et al., 2016).

HY-2A (Haiyang-2A), launched in August 2011, is China's first marine dynamic environment exploration satellite. The HY-2A satellite onboard a dual-frequency (Ku and C-band) radar altimeter first flew on a 14-day near-repeat polar sun-synchronous orbit with a mean altitude of 971 km. On March 23, 2016, HY-2A satellite shifted to the drift orbit with a cycle of 168 days for precise measurement of the geoid. As one of the primary payloads, the HY-2A altimeter has collected more than eight years of data. Many articles had evaluated the data quality of the HY-2A SSH observations and show that the SSH measurements of HY-2A was at almost the same level of accuracy as Jason-2 based on cross-calibration and crossover analysis (Bao et al., 2015;Peng et al., 2015;Yang et al., 2016). HY-2A/ERM data with a high accuracy were used to inverse gravity anomalies in the previous articles (Wan et al., 2017; Guan et al., 2016). Because the ground track spacing is too large (~200 km at the equator), the HY-2A/ERM data were combined with GM data from other satellites to invert gravity anomalies and contributed weakly to the gravity anomaly inversion results.

Unlike the previous ERM data, the HY-2A/GM data with dense ocean coverage have a great potentiality for inversion of the marine gravity field (Zhang et al., 2018). Jiang et al. (2018a) reprocessed HY-2A altimeter sensor geophysical dataset records (SGDR) data and performed a cross-calibration analysis between the reprocessed HY-2A altimeter data and the Jason-2 data. The evaluation showed that the reprocessed HY-2A data were of good

quality and was lower than Jason-2 at the noise level.

In the paper, we focused on the performance of HY-2A/GM data with respect to recovering ocean gravity anomalies. First, the 21 months of reprocessed HY-2A/GM data were used to construct the preliminary ocean gravity anomalies over the waters around Taiwan Island. Then, the preliminary results were analyzed and compared with the marine gravity anomalies derived from CryoSat-2 by the same method. Finally, its performance was verified and evaluated using the global ocean gravity models and National Geophysical Data Center (NGDC) shipboard gravity data.

2 Research area and data

2.1 *Research area*

The gravity field of the sea around Taiwan Island varies widely due to the complex terrain. Because it is close to the Pacific Ocean in the east, the depth reaches more than 4 km near 10–20 km offshore. In the meanwhile time, the adjacent East China Sea, South China Sea and Taiwan Strait have shallow water depth and the relatively flat seabed topography. Besides, the depth of the Taiwan Strait is generally 50 m and there are many small islands in the region. All that provide a good natural test area for altimetry gravity research. Therefore, we selected the area near Taiwan Island (21°–26°N, 119°–123°E) as the research area for the ocean gravity field inversion (Hwang et al., 2006).

2.2 *Data description*

Since the HY-2A satellite entered the drift orbit from the early 14-day repeated orbit in March 2016, geodetic data have been collected for more than three years. The geodetic data with a 168-day repeat cycle has the potentiality to calculate gravity anomalies. Fortunately, we obtained HY-2A SGDR data (including 20 Hz waveform data) from China's National Ocean Satellite Application Service (NSOAS).

Jiang et al. (2018a) reprocessed the HY-2A SGDR data for the two years from January 4, 2014 to January 3, 2016 (cycle 60–111) and compared with the reprocessed Jason-2 radar altimeter data. The ranging and geophysical error correction methods used to reprocess HY-2A and Jason-2 data are shown in Table 1.

Compared with Jason-2, the reprocessed HY-2A altimeter data showed good quality and low noise levels. When the same geophysical correction methods were used to calculate the SSH

for the two missions, the mean standard deviations of the self-crossover differences for HY-2A and Jason-2 are 5.24 cm and 5.34 cm, respectively. These indicate that the SSH measurement of HY-2A has almost the same accuracy as Jason-2 (Jiang et al., 2018a, 2018b). In the same way, the SSH measurement of HY-2A/GM data reprocessed with the same ranging and geophysical error correction terms also has high accuracy.

We selected HY-2/GM SGDR data for nearly 21 months from March 26, 2016 to December 31, 2017, and re-tracked the altimeter waveform using the MLE4 algorithm to obtain a more precise range between the satellite and the sea surface (Wang et al., 2013a, b). And the ranging and geophysical error correction methods shown in Table 1 are used to obtain high-precision SSH measurements.

To date, CryoSat-2 launched by ESA in April 2010 has been collecting about 9 years of geodetic data. The CryoSat-2 geodetic data with a return period of 369 days provided the highest density coverage available today, which is an important dataset for high-resolution global ocean gravity field recovery (Andersen et al., 2015; Sandwell et al., 2013). For comparison, CryoSat-2 sea level anomaly data with the same period of HY-2A were obtained from RADS (http://rads.tudelft.nl). The range and geophysical error corrections for CryoSat-2 data were set as RADS defaults. As can be seen from Table 2, HY-2A has comparable passes with CryoSat-2 at the same time. During the selected period, the number of observation points of CryoSat-2 is 20% more than HY-2A in the research region.

The tracks distribution of HY-2A geodetic mission data near Taiwan Island is shown in Fig. 1a. Figure 1a demonstrates that the geodetic data collected by HY-2A have a dense geographical distribution. For comparison, the distribution of ground tracks of CryoSat-2 in the same period as HY-2A is showed in Fig. 1b. As shown in Fig. 1b, the trajectory of CryoSat-2 is denser than the trajectory of HY-2A/GM in Fig. 1a. This is the fact that the cycle of CryoSat-2 is 369 days, which is more than twice the cycle of HY-2A/GM data. During the selected period, HY-2A/GM ground tracks were repeated about 3 times while the trajectory of CryoSat-2 were only repeated about 1.7 times. Unlike ERM data, their tracks are dense enough to recover high-resolution gravity field by themselves.

3 Methodology

The methods for retrieving ocean gravity anomalies from

Table 1. Models and methods used to reprocess the data of HY-2A and Jason-2 altimeters

Correction	Reprocessed HY-2A	Reprocessed Jason-2
Orbits	SGDR	GDR-D
Range	MLE4	MLE4 in GDR
Dry troposphere correction	ERA-interim	ERA-interim
Wet troposphere correction	ERA-interim	ERA-interim
Ionospheric correction	Filtered dual-frequency ionospheric correction	Filtered dual-frequency ionospheric correction
Sea state bias correction	Non-parametric model	Non-parametric model
Geocentric ocean tide correction	GOT4.10	GOT4.10
Solid earth tide correction	Cartwright and Edden	Cartwright and Edden
Pole tide correction	Wahr	Wahr
Dynamical atmospheric correction	AVISO	AVISO

Table 2. The statistical information of HY-2A/GM and CryoSat-2 data near Taiwan Island

Mission	Cycle/d	No. passes	No. points	Data duration
HY-2A/GM	168	258	10 609	2016-03-26–2017-12-31
CryoSat-2	369	237	12 085	2016-03-28–2018-01-09
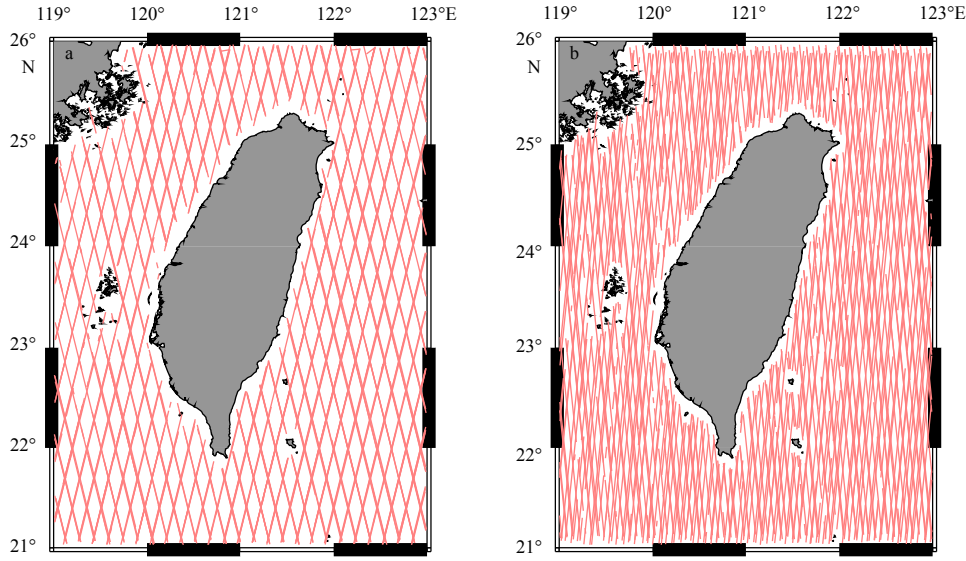
Fig. 1. Distribution of HY-2A/GM (a) and CryoSat-2 (b) ground tracks around Taiwan Island.

satellite altimeter data can be broadly divided into two types: the geoid method and the deflection of the vertical (DOV) method. They are based on geoid heights and geoid gradients, which are obtained by removing the effects of sea surface topography on the sea surface height and sea surface gradients, respectively. Unlike the geoid method, the DOV method can suppress the long-wavelength radial orbit error below the noise level of the altimeter by simply taking the along-track geoid gradients. The tedious crossover adjustment required for the geoid method is eliminated in the DOV method. Besides, many long-wavelength system errors are also attenuated in the DOV method, such as atmospheric propagation errors, ocean circulation, tidal errors, etc. The geoid gradient contains rich high-frequency information, which is beneficial to the inversion of high-resolution ocean gravity field. Therefore, the DOV method is widely used in many articles (Sandwell et al., 1997, 2009; Hwang, 1998; Hwang et al., 2002; Hsiao et al., 2016; Zhang et al., 2017). Sandwell(1992) derived the equations for gravity anomalies and the geoid gradients based on Laplace's equation with a flat-earth approximation and then used the Fast Fourier Transform (FFT) to solve gravity anomalies in the spectrum. The Sandwell's algorithm omits the difference between gravity anomaly and disturbance gravity. Hwang(1998) inverted gravity anomalies from the DOV by the Inverse Vening Meinesz (IVM) formula with a one-dimensional(1-D)FFT method. Since the 1-D FFT method considers the difference in calculating the latitude of the spherical surface, the Hwang's algorithm is more theoretically tight. The DOV method based on the IVM formula was used in the paper for recovering marine gravity anomalies from satellite altimeters.

3.1 *Computing along-track residual DOV*

In the paper, we calculate the DOV by the slope of two successive geoid heights N_1 and N_2 along the track as

$$\varepsilon = \frac{N_2 - N_1}{d},\tag{1}$$

where ε is the DOV, whose geographic location is the mean location of the two geoid heights; d is the point spacing. The estimated standard deviation of ε can be expressed as

$$\sigma_\varepsilon = \frac{\sqrt{\sigma_1^2 + \sigma_2^2}}{d},\tag{2}$$

where σ_1 and σ_2 are respectively the standard deviations of N_1 and N_2.

In order to get really geoid heights, the impact of sea surface topography between SSH and geoid should be receded. However, the sea surface topography can not be modeled accurately. It usually divided into the mean dynamic topography and time-dependent sea surface topography. In general, the average dynamic sea surface topography effect was removed by selecting the appropriate mean dynamic topography model, while the time-varying sea surface topography was treated as high frequency noise (Hwang et al., 2002). The remove-restore method was used in the derivation of gravity anomalies with global gravity model EGM2008 as the reference model. The gravity field model EGM2008 with 5′×5′ resolution, complete to spherical harmonic degree 2 160 (Pavlis et al., 2012), was often used as reference gravity model in recent articles (Sandwell et al., 2014; Hsiao et al., 2016; Zhang et al., 2017). During the actual procedure, the SSHs were differentiated along the track, then along-track residual geoid gradients were obtained by subtracting the slope of the reference geoid derived from EGM2008 gravity model and RIO 05 mean dynamic topography model.

3.2 *Gridding DOV*

The DOV method for inverting ocean gravity anomalies based on the IVM formula requires the use of a one-dimensional FFT method. The FFT method is used on a gauge grid with fixed latitude and longitude spacing. Therefore, it is necessary to grid the along-track DOV before inversion. After removing outliers, the method of least squares collocation was used to compute the north and east components of the deflection of the vertical on a regular grid with 1′×1′ resolution.

3.3 *Computing gravity anomalies*

During a remove-restore procedure, the gravity anomalies were computed from gridded north and east residual geoid gradients by the IVM formula using the gradient of the kernel function H. The IVM formula can be presented as

$$\Delta g_p = \frac{\gamma_0}{4\pi} \iint\limits_{\sigma} (\xi_q \cos \alpha_{qp} + \eta_q \sin \alpha_{qp}) H' \mathrm{d}\sigma_q, \qquad (3)$$

where Δg_p is gravity anomaly at the calculation point p; γ_0 is the mean gravity; α_{qp} is the azimuth from the flow point q to the calculation point p; ξ_q and η_q are the north and east components of the deflection of the vertical, which has the opposite sign to geoid gradient; σ_q is the unit sphere; and H' is the derivative of the Vening Meinesz kernel function H and is defined as

$$H' = \frac{dH}{d\Psi_{qp}} = -\frac{\cos\frac{\Psi_{qp}}{2}}{2\sin^2\frac{\Psi_{qp}}{2}} + \frac{\cos\frac{\Psi_{qp}}{2}\left(3 + 2\sin\frac{\Psi_{qp}}{2}\right)}{2\sin\frac{\Psi_{qp}}{2}\left(1 + \sin\frac{\Psi_{qp}}{2}\right)}, \qquad (4)$$

where Ψ_{qp} is the spherical distance from the flow point q to the calculation point p. When the flow point and the calculation point coincide, the kernel function will be singular. The contribution of the innermost zone to the gravity anomaly should also be considered. The detailed process of the Hwang's algorithm was introduced in these articles (Hwang, 1998; Hwang et al., 1998). Finally, the reference gravity model EGM2008 was added back to the gravity anomalies to establish the 1′×1′ marine gravity grids near Taiwan Island.

4 Results and discussion

4.1 *Gravity inversion results*

According to the above method, we transformed along-track geoid slope derived from HY-2A/GM into marine gravity anomalies with a resolution of 1′×1′. To validate the HY-2A gravity anomalies retrievals, the gravity anomalies were inverted by CryoSat-2 data with the same period of HY-2A in the same way. The statistical information of gravity anomalies derived from HY-2A and CryoSat-2 data near Taiwan Island as shown in Table 3. The mean of the ocean results derived from HY-2A and CryoSat-2 are respectively 9.005 mGal and 9.018 mGal, while their standard deviations (STD) are 61.371 mGal and 61.302 mGal, respectively. Besides, the mean values of their gravity anomalies are almost equal and the gravity anomaly grid difference has an STD of 3.699 mGal. As shown in Fig. 2, a good agreement between the two data sets is found, which verifies that the performance of HY-2A is similar to CryoSat-2 with respect to recovering marine gravity anomalies.

Figure 3a demonstrates the marine gravity field from the 21 months of HY-2A geodetic data near Taiwan Island. The inversion results in the study area are within [–250, 350] mGal, and 99% of the values are concentrated in the range of ±250 mGal. In order to display the details better, ±250 mGal is selected as the color scale range. The gravity anomaly is very obvious: the eastern region is shown in dark blue, while the southeast region is shown in orange. This is because the east side of Taiwan Island is close to the steep Pacific Ocean and there are several small islands in the southeast. In addition, most of the western and

Table 3. The statistical information of HY-2A/GM and CryoSat-2 gravity anomaly recovery near Taiwan Island

Dataset	Min /mGal	Max /mGal	Mean /mGal	STD /mGal
HY-2A/GM	−240.670	344.758	9.005	61.371
Cryosat-2	−232.441	345.659	9.018	61.302
HY-2A/GM vs Cryosat-2	−13.948	13.924	−0.028	3.699
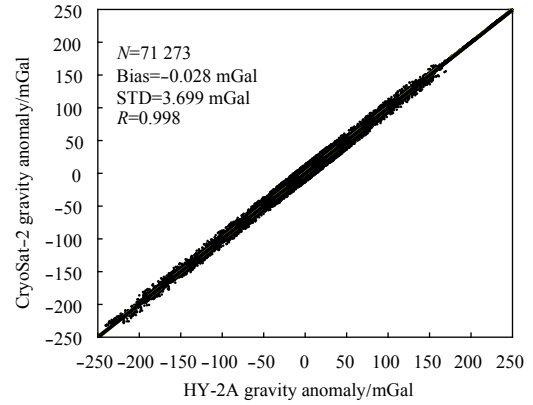
**Fig. 2.** Scatterplot of HY-2A gravity anomaly versus CryoSat-2 gravity anomaly near Taiwan Island.

northern regions are covered by green, due to the flat seabed of the East China Sea and the Taiwan Strait. The light blue of the southwest is caused by the deep sea of the South China Sea. The gravity anomaly from HY-2A is highly matched with the complex terrain of the study area, which verifies the validity of the preliminary results.

The gravity field inverted by CryoSat-2 data in the same way is presented in Fig. 3b. Comparing the picture of HY-2A with CryoSat-2, we find that their inversion results show similar gravity anomalies information. However, in the Pacific Ocean to the east of Taiwan Island and the adjacent waters southeast of Taiwan Island, there are some small discrepancies between the two results. Because the trajectory of HY-2A is relatively sparse, the difference between the two figures may come from the interpolation error of HY-2A. It is also possible that HY-2A's unique trajectory allows it to obtain more terrain information. Whether the discrepancies are due to noise or terrain details is an interesting issue worthy of further study.

4.2 *Comparisons with global gravity models*

To compare the performance of the gravity anomalies derived from HY-2A/GM and CryoSat-2, we first focused on the existing global gravity models, such as EGM2008, DTU13 (Andersen et al., 2014) and V23.1 (Sandwell et al., 2014). A point-wise comparison between the inversion results and the existing global marine gravity models around Taiwan Island is shown in Table 4. The mean values of the differences are within 0.118 mGal. For HY-2A and CryoSat-2, the STD values of the differences between the inversion results and DTU13 are 3.458 mGal and 3.229 mGal, respectively, while they against V23.1 are 5.274 mGal and 5.129 mGal, respectively. With EGM2008 as a standard reference, the STD values are 3.257 mGal and 2.685 mGal respectively. Comparisons with the three global marine gravity field model indicates that HY-2A and CryoSat-2 are at the same level in terms of gravity field inversion. For both HY-2A and CryoSat-2, we find that the mean and STD values of the differences against V23.1 are greater than DTU13 and EGM2008. This may be because the value of V23.1 represents disturbing gravity, which is slightly larger than the gravity anomalies derived from DTU13 and EGM2008.

Scatterplots of HY-2A gravity anomaly and CryoSat-2 gravity anomaly versus the global marine gravity models near Taiwan Island is shown in Fig.4. We can see that the inversion results have a high coherence coefficient with the global gravity field models, and HY-2A and CryoSat-2 have high consistency with the same global ocean gravity field model.
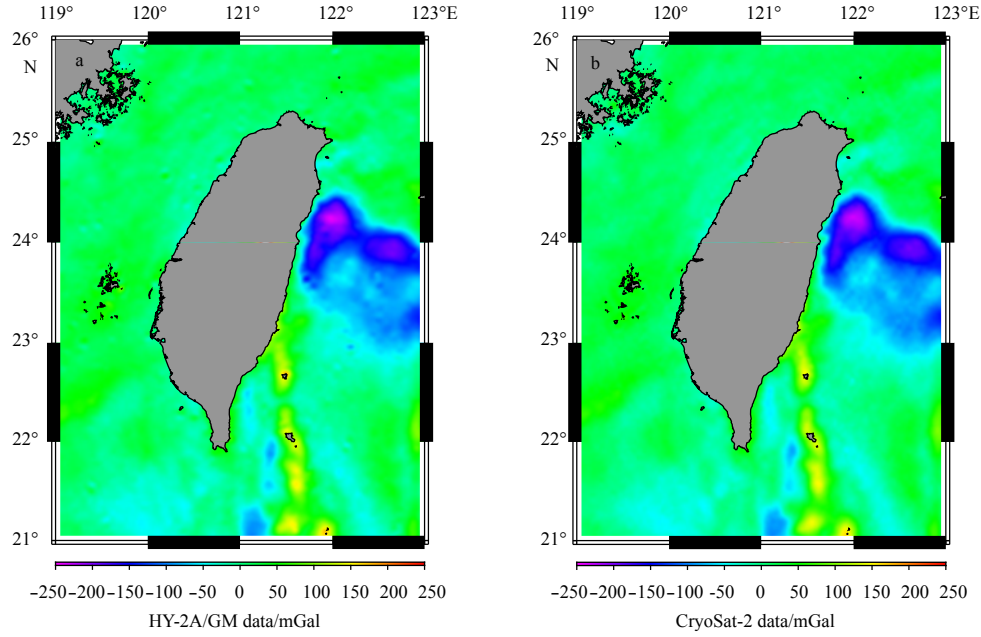
Fig. 3. Marine gravity field from HY-2A/GM data (a) and CryoSat-2 data (b) near Taiwan Island.

Table 4. The point-wise comparison between the inversion results and global marine gravity models near Taiwan Island

Model description	Mean/mGal	STD/mGal
HY-2A/GM vs EGM2008	0.008	3.257
CryoSat-2 vs EGM2008	−0.021	2.685
HY-2A/GM vs DTU13	0.042	3.458
CryoSat-2 vs DTU13	−0.008	3.229
HY-2A/GM vs V23.1	0.118	5.274
CryoSat-2 vs V23.1	0.086	5.129

4.3 *Verification against NGDC shipboard gravity*

Considering that the STD σ_{HC} of the differences between HY-2A and CryoSat-2 is 3.699 mGal, the verification using ship gravity data will be our next step. The US NGDC provides globally distributed shipboard data and there are 42 tracks near Taiwan as shown in Fig.5.

In order to make the verification of the shipboard gravity data more reliable, it is necessary to remove the systematic deviation and outliers of the shipboard data. The shipboard data were initially evaluated with EGM2008, and the threshold of 20 mGal results in the deletion of 3.71% of the total data. Considering the sparse distribution of the shipboard gravity data, the error will be larger if the ship survey data are interpolated to the altimeter-derived gravity grids. Therefore, the satellite and EGM2008 grids were sampled at the shipboard gravity locations resulting in 51 586 points for comparison. Then these shipboard data were used for verification and the verification results are shown in Table 5.

We can see that the STD σ_{HS} is 6.791 mGal for HY-2A vs Shipboard, while the STD σ_{CS} is 6.505 mGal for CryoSat-2 vs Shipboard. The verification indicates further that the inversion results of HY-2A and CryoSat-2 are approximately equivalent against shipboard gravity data. In addition, it can be seen from Fig.6 that in the case of more than 50 000 data points, the HY-2A altimeter-derived gravity data has a coherence coefficient of 0.989 with the ship's measured gravity data. That once again confirms the good performance of HY-2A in the recovery of gravity field. It might be argued that the comparison with shipboard gravity data is not impressive giving STD around 7 mGal. The reason is the fact that the shipboard data used for verification is only simply preprocessed and still contains large noises. In addition, the gravity field variation around Taiwan is greatly large. The STD of the gravity anomalies in the region is 61 mGal compared with 27 mGal as the global number.

4.4 *Gravity field assessment*

To establish the noise contributions of these two gravity grids derived from HY-2A and CryoSat-2, the independent data from a shipboard gravity survey were used. Using the three-way variance approach described in the paper (Sandwell et al., 2013), we assess the STD of three independent marine gravity data sets for the research area. The first data set is the gravity data set derived from HY-2A altimeter, which is based on the first 21 months of GM data from March 26, 2016 to December 31, 2017. The second data set is the CryoSat-2 altimeter-derived gravity data set, which is based on the GM data with the same period of HY-2A. The third is shipboard gravity data from the NGDC, which contains all 42 tracks near Taiwan. Assuming the error sources in each data set are statistically independent, one can write the variance of the point-wise differences in terms of the individual variances as follows:

$$\begin{bmatrix} \sigma_{HS}^2 \\ \sigma_{CS}^2 \\ \sigma_{HC}^2 \end{bmatrix} = \begin{bmatrix} 1 & 0 & 1 \\ 0 & 1 & 1 \\ 1 & 1 & 0 \end{bmatrix} \begin{bmatrix} \sigma_H^2 \\ \sigma_C^2 \\ \sigma_S^2 \end{bmatrix}. \tag{5}$$

Based on the Eq. (5), we can calculate estimates of the individual standard deviations of $\sigma_H = 2.957$ mGal; $\sigma_C = 2.223$ mGal; $\sigma_S = 6.114$ mGal. The analysis indicates that the inversion results of HY-2A have slightly worse precision than the CryoSat-2. Moreover, their satellite gravity data are much better than the shipboard gravity data.

Assessing the accuracy of the satellite gravity requires a com-
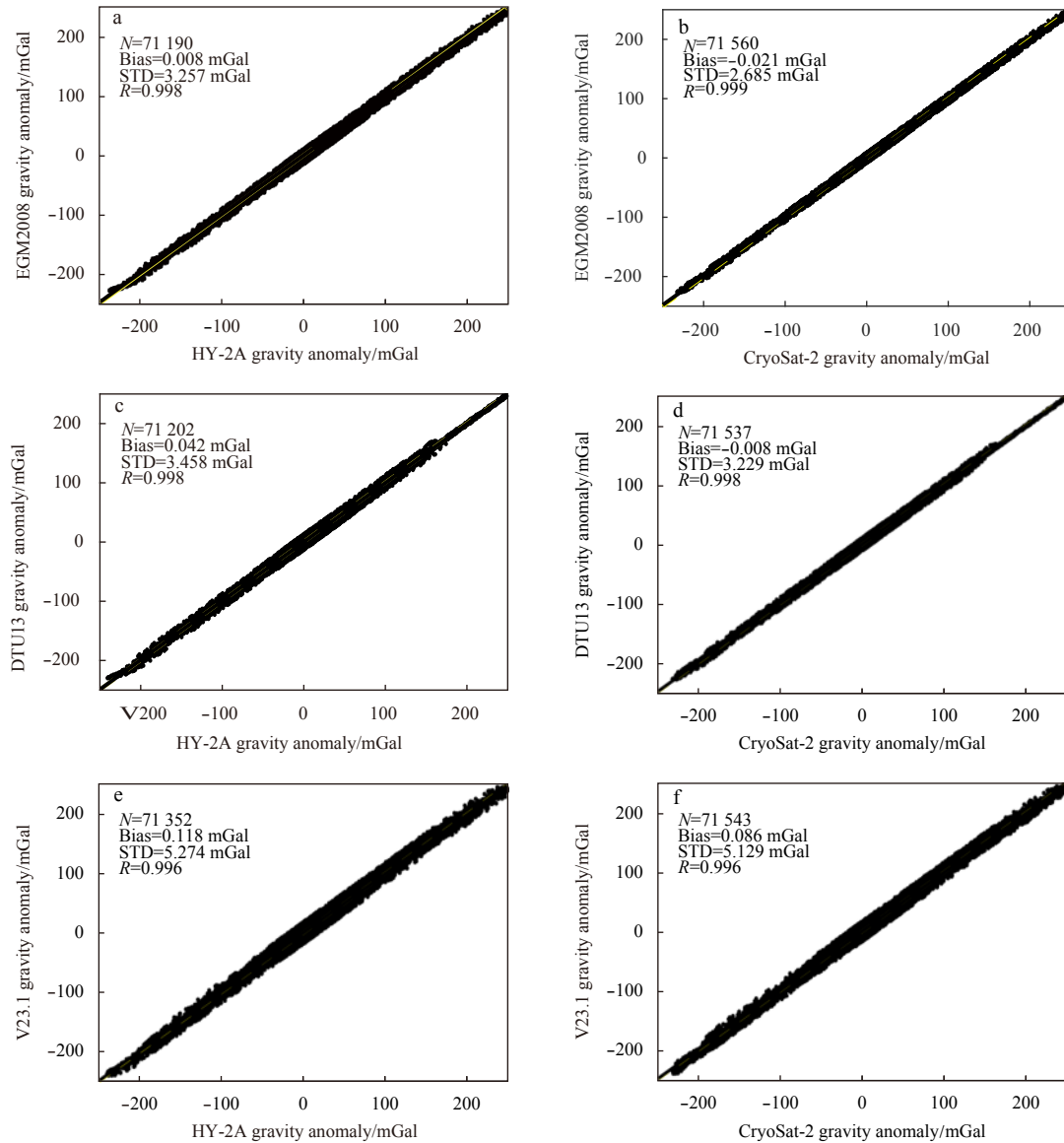
Fig. 4. Scatterplots of HY-2A gravity anomaly (a, c, e) and CryoSat-2 gravity anomaly （b, d, f） versus the global marine gravity models near Taiwan Island.

parison with more accurate data. Therefore, the data from integrated gravity field model EGM2008 with 5′×5′ resolution are more suitable than the sparse shipboard gravity data to evaluate the accuracy of HY-2A and CryoSat-2 gravity. As shown in Table 4, the HY-2A to EGM2008 STD σ_{HE} is 3.257 mGal while the CryoSat-2 to EGM2008 STD σ_{CE} is 2.685 mGal. Besides, the HY-2A to CryoSat-2 STD σ_{HC} still is 3.699 mGal. Just like the above analysis, we can get estimates of the individual standard deviations of σ_{H}= 2.922 mGal; σ_{C}=2.268 mGal; σ_{E}= 1.438 mGal. The analysis shows that the EGM2008 data really are much better than the other satellite data. Compared with NGDC to evaluate the results, the accuracy of the gravity fields of HY-2A and CryoSat-2 is basically unchanged, which also confirms the credibility of the results. Furthermore, HY-2A and CryoSat-2 are at the same noise level in terms of gravity field inversion and the CryoSat-2 data have slightly better precision than the HY-2A in the case of 20% more observation points in the study area. The current results are based only on the first 21 months of HY-2A/GM data. If HY-2A can collect 15 years of geodetic data, it can achieve a high-preci-
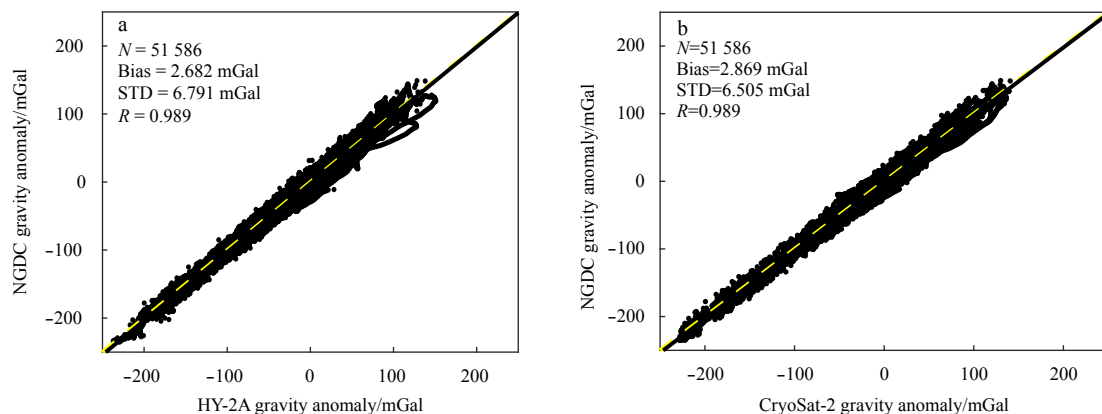
sion gravity field of 1 mGal.

5 Summary and conclusions

Since HY-2A entered the drift orbit in March 2016, more than three years of geodetic data have been collected. The paper presents the preliminary marine gravity field derived from HY-2A/GM data around Taiwan Island. From the preliminary results of HY-2A, the complex gravity field distribution near Taiwan Island is clearly displayed. Comparing with the gravity anomalies from the CryoSat-2 data by the same method, these two data sets are highly matched. Compared with the gravity data of EGM2008, DTU13, V23.1 and NGDC, HY-2A has similar performance to CryoSat-2 in recovering ocean gravity anomalies. These results show the potentiality for HY-2A to inverse high-resolution gravity anomalies.

The independent data from NGDC shipboard gravity survey and EGM2008 gravity are used to assess the preliminary marine gravity fields derived from HY-2A/GM and CryoSat-2 data for the research area. Regardless of NGDC or EGM2008, the accuracy of
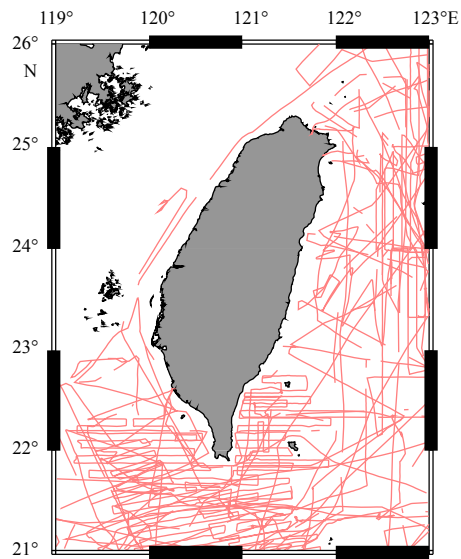
Fig. 5. Trajectory of NGDC ship-measured gravity data near Taiwan Island.

Table 5. Validation information with NGDC shipboard gravity data near Taiwan Island

Model description	mean/mGal	STD/mGal
HY-2A/GM vs Shipboard	2.682	6.791
CryoSat-2 vs Shipboard	2.869	6.505
EGM2008 vs Shipboard	2.859	6.020

the gravity field of HY-2A and CryoSat-2 is basically the same. The marine gravity field derived from the first 21-month HY-2A/GM data has an accuracy of 2.922 mGal. After 15 years of geodetic data collection, HY-2A has the potential to invert 1 mGal high-resolution ocean gravity field.

At present, it is only the preliminary inversion result. The refined processing can further reduce the noise error and improve the inversion accuracy, such as optimized re-tracking method (Guo et al., 2010; Yang et al., 2012; Garcia et al., 2014), filtering and resampling procedure (Zhang et al., 2017), etc. Nowadays, the data from HY-2A altimeter are mainly processed and evaluated in the coastal regions. In the future, we will process the data in the open ocean, inland and ice sheet and compare the data with some other altimeters such as Jason-2 and SARAL/AltiKa.

Fig. 6. Scatterplots of HY-2A gravity anomaly (a) and CryoSat-2 gravity anomaly (b) versus NGDC shipboard gravity data near Taiwan Island.

References

Andersen O B, Knudsen P. 1998. Global marine gravity field from the ERS-1 and Geosat geodetic mission altimetry. Journal of Geophysical Research, 103(C4): 8129–8137, doi: 10.1029/97JC02198

Andersen O B, Knudsen P, Berry P A M. 2010. The DNSC08GRA global marine gravity field from double retracked satellite altimetry. Journal of Geodesy, 84(3): 191–199, doi: 10.1007/s00190-009-0355-9

Andersen O B, Knudsen P, Kenyon S, et al. 2014. Global and arctic marine gravity field from recent satellite altimetry (DTU13). In:

Proceedings of the 76th EAGE Conference and Exhibition. Amsterdam: European Association of Geoscientists & Engineers

Andersen O B, Jain M, Knudsen P. 2015. The impact of using jason-1 and cryosat-2 geodetic mission altimetry for gravity field modeling. In: Rizos C, Willis P, eds. IAG 150 Years. Cham: Springer, 205–210, doi: 10.1007/1345_2015_95

Bao Lifeng, Gao Peng, Peng Hailong, et al. 2015. First accuracy assessment of the HY-2A altimeter sea surface height observations: cross-calibration results. Advances in Space Research, 55(1): 90–105, doi: 10.1016/j.asr.2014.09.034

Garcia E S, Sandwell D T, Smith W H F. 2014. Retracking CryoSat-2, Envisat and Jason-1 radar altimetry waveforms for improved gravity field recovery. Geophysical Journal International, 196(3): 1402–1422, doi: 10.1093/gji/ggt469

Guan Yihe, Sheng Hui, Liu Shanwei, et al. 2016. Inversion of the gravity anomalies by using multi-generation satellite altimeter data in the South China Sea. Hydrographic Surveying and Charting (in Chinese), 36(1): 11–14

Guo Jinyun, Gao Yonggang, Hwang C, et al. 2010. A multi-subwaveform parametric retracker of the radar satellite altimetric waveform and recovery of gravity anomalies over coastal oceans. Science China Earth Sciences, 53(4): 610–616, doi: 10.1007/s11430-009-0171-3

Haxby W F, Karner G D, Labrecque J L, et al. 1983. Digital images of

combined oceanic and continental data sets and their use in tectonic studies. EOS, Transactions American Geophysical Union, 64(52): 995–1004, doi: 10.1029/EO064i052p00995

Hsiao Y S, Hwang C, Cheng Y S, et al. 2016. High-resolution depth and coastline over major atolls of South China Sea from satellite altimetry and imagery. Remote Sensing of Environment, 176: 69–83, doi: 10.1016/j.rse.2016.01.016

Hwang C. 1998. Inverse Vening Meinesz formula and deflection-geoid formula: applications to the predictions of gravity and geoid over the South China Sea. Journal of Geodesy, 72(5): 304–312, doi: 10.1007/s001900050169

Hwang C, Guo J Y, Deng X L, et al. 2006. Coastal gravity anomalies from retracked Geosat/GM altimetry: improvement, limitation and the role of airborne gravity data. Journal of Geodesy, 80(4): 204–216, doi: 10.1007/s00190-006-0052-x

Hwang C, Hsu H Y, Jang R J. 2002. Global mean sea surface and marine gravity anomaly from multi-satellite altimetry: applications of deflection-geoid and inverse Vening Meinesz formulae. Journal of Geodesy, 76(8): 407–418, doi: 10.1007/s00190-002-0265-6

Hwang C, Kao E C, Parsons B. 1998. Global derivation of marine gravity anomalies from Seasat, Geosat, ERS-1 and TOPEX/POSEIDON altimeter data. Geophysical Journal International, 134(2): 449–459, doi: 10.1111/j.1365-246X.1998.tb07139.x

Jiang Maofei, Xu Ke, Liu Yalong. 2018a. Global Statistical Assessment and Cross-Calibration with Jason-2 for Reprocessed HY-2A Altimeter Data. Marine Geodesy, 41(3): 289–312, doi: 10.1080/01490419.2017.1375053

Jiang Maofei, Xu Ke, Liu Yalong, et al. 2018b. Assessment of reprocessed sea surface height measurements derived from HY-2A radar altimeter and its application to the observation of 2015-2016 El Niño. Acta Oceanologica Sinica, 37(1): 115–129, doi: 10.1007/s13131-018-1162-z

McAdoo D C, Marks K M. 1992. Gravity fields of the southern ocean from Geosat data. Journal of Geophysical Research: Solid Earth, 97(B3): 3247–3260, doi: 10.1029/91JB02797

Pavlis N K, Holmes S A, Kenyon S C, et al. 2012. The development and evaluation of the earth gravitational model 2008 (EGM2008). Journal of Geophysical Research: Solid Earth, 117(B4): B04406

Peng Hailong, Lin Mingsen, Mu Bo, et al. 2015. Global statistical evaluation and performance analysis of HY-2A satellite radar altimeter data. Haiyang Xuebao (in Chinese), 37(7): 54–66

Rapp R H. 1979. Geos 3 data processing for the recovery of geoid undulations and gravity anomalies. Journal of Geophysical Research: Solid Earth, 84(B8): 3784–3792, doi: 10.1029/JB084iB08p03784

Rapp R H. 1986. Gravity anomalies and sea surface heights derived from a combined GEOS 3/Seasat altimeter data set. Journal of Geophysical Research: Solid Earth, 91(B5): 4867–4876, doi: 10.1029/JB091iB05p04867

Sandwell D T. 1992. Antarctic marine gravity field from high-density satellite altimetry. Geophysical Journal International, 109(2): 437–448, doi: 10.1111/j.1365-246X.1992.tb00106.x

Sandwell D, Garcia E, Soofi K, et al. 2013. Toward 1-mGal accuracy in global marine gravity from Cryosat-2, Envisat, and Jason-1. The Leading Edge, 32(8): 892–899, doi: 10.1190/tle32080892.1

Sandwell D T, McAdoo D C. 1988. Marine gravity of the southern ocean and Antarctic margin from Geosat. Journal of Geophysical Research: Solid Earth, 93(B9): 10389–10396, doi: 10.1029/JB093iB09p10389

Sandwell D T, Müller R D, Smith W H F, et al. 2014. New global marine gravity model from CryoSat-2 and Jason-1 reveals buried tectonic structure. Science, 346(6205): 65–67, doi: 10.1126/science.1258213

Sandwell D T, Smith W H F. 1997. Marine gravity anomaly from Geosat and ERS 1 satellite altimetry. Journal of Geophysical Research: Solid Earth, 102(B5): 10039–10054, doi: 10.1029/96JB03223

Sandwell D T, Smith W H F. 2009. Global marine gravity from retracked Geosat and ERS-1 altimetry: ridge segmentation versus spreading rate. Journal of Geophysical Research: Solid Earth, 114(B1): B01411

Wan Jianhua, Li Ruizhou, Liu Shanwei, et al. 2017. Effection analysis for gravity precision from HY-2A altimeter data. Hydrographic Surveying and Charting (in Chinese), 37(4): 24–27

Wang Lei, Xu Ke, Liu Peng, et al. 2013a. An echo model for big antenna mispointing angle and its application in HY-2A satellite radar altimeter. Acta Electronica Sinica (in Chinese), 41(9): 1836–1841

Wang Lei, Xu Ke, Xu Xiyu, et al. 2013b. A new method for computing radar altimeter look-up correction table and its application. Journal of Electronics & Information Technology (in Chinese), 35(4): 908–914

Yang Yuande, Hwang C, Hsu H J, et al. 2012. A subwaveform threshold retracker for ERS-1 altimetry: a case study in the Antarctic Ocean. Computers & Geosciences, 41: 88–98

Yang Lei, Zhou Xinghua, Lin Mingsen, et al. 2016. Global statistical assessment of HY-2A altimeter IGDR data. Progress in Geophysics (in Chinese), 31(2): 629–636

Zhang Shengjun, Li Jiancheng, Jin Taoyong, et al. 2018. HY-2A altimeter data initial assessment and corresponding two-pass waveform Retracker. Remote Sensing, 10(4): 507, doi: 10.3390/rs10040507

Zhang Shengjun, Sandwell D T, Jin Taoyong, et al. 2017. Inversion of marine gravity anomalies over southeastern China seas from multi-satellite altimeter vertical deflections. Journal of Applied Geophysics, 137: 128–137, doi: 10.1016/j.jappgeo.2016.12.014